Optoelectronic Digital Capture Device Based on Si/C Multilayer Heterostructures

Conference Paper *in* IFIP Advances in Information and Communication Technology · April 2013

DOI: 10.1007/978-3-642-37291-9_60

CITATIONS
4

READS
10

5 authors, including:

Vitor Vaz da Silva
Instituto Politécnico de Lisboa
71 PUBLICATIONS **328** CITATIONS
SEE PROFILE

Manuel Augusto Vieira
Instituto Politécnico de Lisboa
74 PUBLICATIONS **190** CITATIONS
SEE PROFILE

Paula Louro
Instituto Politécnico de Lisboa
227 PUBLICATIONS **903** CITATIONS
SEE PROFILE

Manuela Vieira
Instituto Politécnico de Lisboa
419 PUBLICATIONS **1,918** CITATIONS
SEE PROFILE

Optoelectronic Digital Capture Device Based on Si/C Multilayer Heterostructures

Vitor Silva[1,2], Manuel A. Vieira[1,2], Paula Louro[1,2], Manuela Vieira[1,2,3], and Manuel Barata[1,2]

[1] Electronics Telecommunications and Computer Dept, ISEL, Lisbon, Portugal
[2] CTS-UNINOVA, Quinta da Torre, 2829-516, Caparica, Portugal
[3] DEE-FCT-UNL, Quinta da Torre, 2829-516, Caparica, Portugal

Abstract. Combined tunable WDM converters based on SiC multilayer photonic active filters are analyzed. The operation combines the properties of active long-pass and short-pass wavelength filter sections into a capacitive active band-pass filter. The sensor element is a multilayered heterostructure produced by PE-CVD. The configuration includes two stacked SiC p-i-n structures sandwiched between two transparent contacts. Transfer function characteristics are studied both theoretically and experimentally. Results show that optical bias activated photonic device combines the demultiplexing operation with the simultaneous photodetection and self amplification of an optical signal acting the device as an integrated photonic filter in the visible range. Depending on the wavelength of the external background and irradiation side, the device acts either as a short- or a long-pass band filter or as a band-stop filter. The output waveform presents a nonlinear amplitude-dependent response to the wavelengths of the input channels. A numerical simulation and a two building-blocks active circuit is presented and gives insight into the physics of the device.

Keywords: SiC hetrostructures, Optical sensors, Optical active filters, Numerical and electrical simulations, Optoelectronic model.

1 Introduction

An optoelectronic device converts light photons to electrons that mimic the light signal in such way that data transmitted by the light beam can be received and processed further with electrical circuits. These devices have one surface over which the optical signal shines. On our device, a multilayered Si/C heterostructure [1, 2], light can shine on the two surfaces, namely back and front. This device acts as an optical filter when other fixed wavelengths superimpose the incident light data signal on the surface it shines with. By selecting a wavelength on either the red or blue part of the spectrum the device can be tuned as a filter and used as a wavelength division multiplexing-demultiplexing technique, WDM [3]. This device has been characterized with a model with its experimental verification. This paper continues this work by analyzing the digital signals which modulate the incident light beam and performs logic functions [4, 5].

L.M. Camarinha-Matos, S. Tomic, and P. Graça (Eds.): DoCEIS 2013, IFIP AICT 394, pp. 555–562, 2013.

2 Internet of Things

Internet is a well known concept that reflects the whole connection of computers forming a single international network. Behind computers are users and their communication skills looked upon this network as an excellent communication media for human interaction and thus the social network bruited. People while communicating with one another usually share ideas, emotions and objects as photographs, text, sound, video, and much more things could be handled. The Internet of Things is a growing concept since Kevin Ashton brought it forward in 1999[6]. Objects are easily identified when an RFID tag is attached to them, and its whereabouts can be known. But objects don't actually communicate. Were this possible and an Internet of physical objects can emerge. People and objects interacting; whoever leaves its home keys inside the house would not be locked outside but instead a warning signal from the keys would call to ones attention. The umbrella would also call to its attention if the weather report expects rain. An occasional party could be foreseen in the agenda and tagged clothes would shine a few leds indicating possible matches inside the cupboard and eventually for the couple, even if they were in different homes. The device we propose would certainly be integrated in objects of design which interact with people via colored visible light.

3 Device Optimization and Characterization

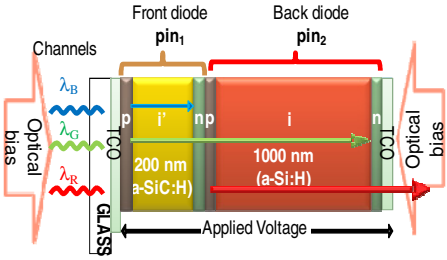

Fig. 1. Device configuration and operation

The sensor element is a multilayered heterostructure based on a-Si:H and a-SiC:H. The configuration shown in Fig. 1 includes two stacked p-i-n structures sandwiched between two transparent contacts. The thicknesses and optical gap of the front í'- (200nm; 2.1 eV) and back i- (1000nm; 1.8eV) layers are optimized for light absorption in the blue and red ranges, respectively.

Spectral response measurements without and under different optical bias and frequencies were performed in order to test the devices sensitivity.

The device operates within the visible range using as input color channels (data) the wave square modulated light (external regulation of frequency and intensity) supplied by a red (624 nm; 51 μW/cm^2), a green (526 nm; 73 μW/cm^2) and a blue (470 nm; 115 μW/cm^2) LED. Additionally, steady state violet (400 nm, 2800 μW/cm^2), red (624 nm, 652 μW/cm^2), green (526 nm, 580 μW/cm^2) and blue (470 nm, 680 μW/cm^2)

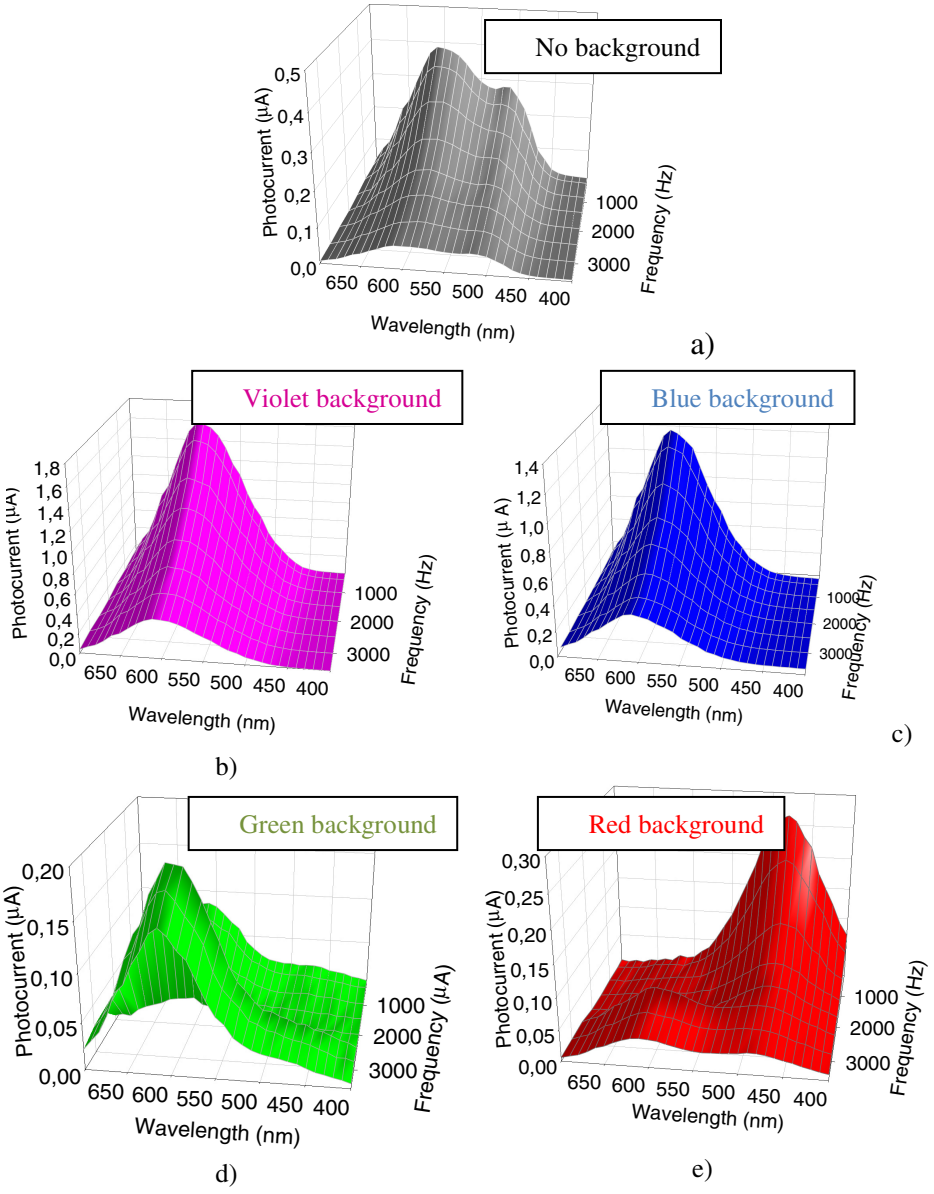

Fig. 2. Spectral photocurrent without (a) and under violet (b), blue (c), green (d) and red (e) bias control applied from the front side

illumination (optical bias) was superimposed from the front (pin_1) and back (pin_2) sides, in LEDs driven at different current values.

The spectral sensitivity was analyzed by applying different wavelengths optical bias from the front and back sides of the device (see Fig.1). Under front irradiation, in Fig. 2 it is displayed the spectral photocurrent for different frequencies without (a)

and under violet (b), blue (c), green (d) and red (e) light bias control at -8V applied voltage and different frequencies (250 Hz-3500Hz).

Results show that the spectral response depends strongly on the bias control wavelength and frequency. As the bias control wavelength increases the spectral sensitivity shifts to the low wavelength spectral regions and decreases with the frequency, suggesting capacitive effect across the device.

In Fig. 3 it is displayed the spectral photocurrent at 3500 Hz, under red, green, blue and violet background irradiations (color symbols) and without it (black symbols) applied from the front (a) and back (b) diodes. For comparison the spectral photocurrent (right axis) for the front, p-i'-n and the back, p-i-n, photodiodes (dash lines) are superimposed.

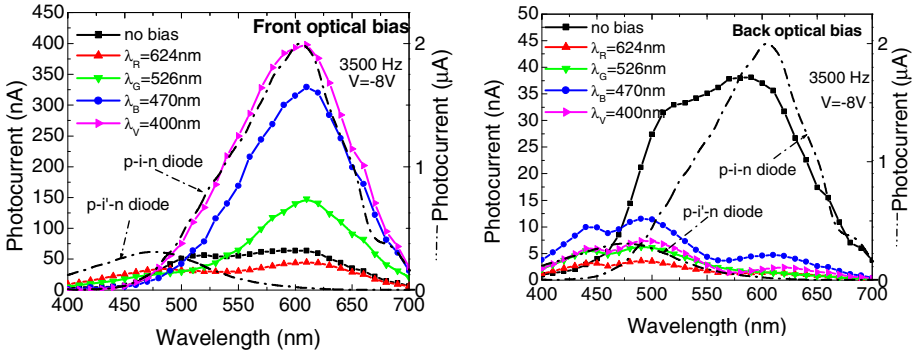

a) b)

Fig. 3. Spectral photocurrent under red, green, blue and violet background irradiations (color symbols) and without it (black symbols) applied from the front (a) and back (b) diodes

Results show that the spectral sensitivity, under steady state irradiation, depends on its wavelength and on the impinging side.

Under front irradiation, the back diode photoresponse is tuned and the sensitivity strongly increases for wavelengths higher than 500 nm when compared with its value without optical bias. Here, as the background wavelength decreases the spectral response increases.

Under back irradiation the front diode photoresponse is selected. The sensitivity strongly increases in the short wavelengths range and collapse in the long wavelength region.

4 Light Filtering Effects

In Fig. 4, at 3500 Hz, it is displayed the ratio between the photocurrent under different optical bias and without it (gain) under front (symbols) and back (lines) irradiations: red (α^R), green (α^G), blue (α^B) and violet (α^V).

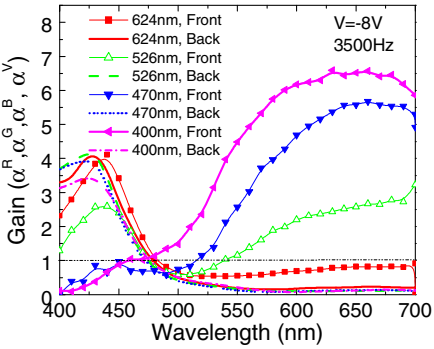

Fig. 4. Gain under front (symbols) and back (lines) irradiations: red (α^R), green(α^G), blue (α^B), violet (α^V)

Under back irradiation (lines) the gain does not depend on the wavelength of the background. The spectral sensitivity in the low wavelength range is enhanced and the device acts, always, as a short-pass filter.

Under front irradiation (symbols) the filter properties of the device depend on the background wavelength. Under red irradiation (Fig. 2e) the gain is high in the short wavelengths range acting the device as a short-pass filter. Under violet (Fig.2b) and blue (Fig.2c) irradiations the transfer function presents an enhanced gain in the long wavelength range acting as a long-pass filter. Under front green background (Fig.2d) the device, for frequencies higher than 2000 Hz, is a band-rejection active filter that works to screen out wavelengths that are within the medium range (475nm-550nm), giving easy passage at all wavelengths below and above.

Results confirm that under controlled wavelength backgrounds it is possible to fine-tune the spectral sensitivity of the device. Its sensitivity is strongly enhanced ($\alpha>1$) in a specific wavelength range and quenched ($\alpha<1$) in the others, tuning or suppressing a specific band. The sensor is a wavelength current-controlled device [7] that makes use of changes in the wavelength and impinging side of the optical bias to control the power delivered to the load. Self optical bias amplification or quenching under uniform irradiation is achieved. By using background lights with complementary light penetration depths across the pi´n/pin device and changing the irradiation side, it is possible to control the spectral response and to filter a specific wavelength band.

5 Research Question and Hypothesis

How many channels in the visible light range can be transmitted by WDM with a a-Si:H and a-SiC:H sensor selecting the desired channel with visible light?

Light shining on one of the surfaces, the selector, can be used to distinguish between two signals with different wavelengths. For n different selecting frequencies there would be 2^n different signals to be identified. Value of n is then limited by the bandwidth of each channel. By changing the wavelength of the selector the output

changes due to the non linear gain of the device which will reduce the maximum number of distinguishable channels. This limitation can be overcome and the number of identifiable channels may increase if the output of the selecting wavelengths are combined with an algorithm and signal modulation. Experimental results are presented in this paper with four different visible leds which are commonly available in the market. These results were obtained with a maximum bit rate of 6000bps. Although this is a very low throughput we are not at this stage worried with this aspect, but to study the recovery of several input signals with only one sensor. In this paper we present the gains of each of the four channels. This represents the influence of each of the selectors upon each input signal wavelength.

6 Photonic Active Filters

To analyze the device under information-modulated wave and uniform irradiation, three monochromatic pulsed lights separately (red, green and blue input channels) or their combination (MUX signal) illuminated the device. Steady state red (652μWcm^{-2}), green (515μWcm^{-2}), blue (680μWcm^{-2}) and violet (2800μWcm^{-2}) optical bias was superimposed separately from the front (pin_1) and the back (pin_2) sides and the photocurrent measured at -8 V.

In Table 1 the gains (α) of the individual channels, defined as the ratio between photocurrents under irradiation (ON state) and without it (OFF state), for the red, green, and blue input channels are presented. Here, the superscripts are related to the background wavelength (R, G, B, V) and the subscripts (R$pin_{1,2}$,G $pin_{1,2}$ B $pin_{1,2}$) to the channel color and irradiation side.

Results show that, even under transient conditions, the effect of the background wavelength and impinging side presents the same nonlinear dependence as in Fig. 4. The morphology of filter results from the interaction of the electric field under applied optical bias (red, green, blue, violet) and the transient electric field induced by the input channels (red, green, blue and violet). Under back irradiation the small absorption depth of the violet photons across the back diode quenches the electric field there and so, the red collection (Red ON) almost disappears ($\alpha^{V}_{R,pin2}<<1$). Blue channel is absorbed across the front diode where the electric field was enhanced resulting in an increase collection of the blue channel ($\alpha^{V}_{B,pin2}>1$). Since the green channel is absorbed across front and back diodes its collection is balanced by the increase collection in the front diode and its reduction at the back ($\alpha^{V}_{G,pin2}\sim1$). The front violet background is absorbed at the surface of the front diode, increasing the electric field at the back diode, where the red and part of the green channels generate optical carriers. So, the collection is strongly enhanced ($\alpha^{V}_{R,pin1}>>1$, $\alpha^{V}_{G,pin1}>1$) while the blue collection stays near its dark value ($\alpha^{V}_{B,pin1}\sim1$).

Polychromatic combinations of the same red, green, blue and violet input channels whose gain is presented in Table I was used to generate a multiplexed (MUX) signal.

In Fig. 5 the filtered signals under front (pin_1) and back (pin_2) violet light control are displayed. The signals were normalized to the maximum intensity under violet front irradiations to suppress the dependence on sensor and LEDs positioning. The bit sequences used to transmit the information are shown at the top of the figures.

Table 1. Gains ($\alpha^{R,G,B,V}_{R,G,B,pin1,2}$) at the input red, green, and blue channels wavelengths

Channels	α^R	α^G	α^B	α^V
$\alpha_{R,pin1}$	0,62	1,28	3,00	5,13
$\alpha_{R,pin2}$	0,12	0,42	0,47	0,34
$\alpha_{G,pin1}$	0,63	0,85	1,52	2,40
$\alpha_{G,pin2}$	0,59	0,62	0,67	0,67
$\alpha_{B,pin1}$	1,39	1,00	0,81	1,11
$\alpha_{B,pin2}$	2,22	1,94	1,97	1,64
$\alpha_{V,pin1}$	11,57	5,80	1,60	1.00
$\alpha_{V,pin2}$	11,57	13,90	1,20	10,42

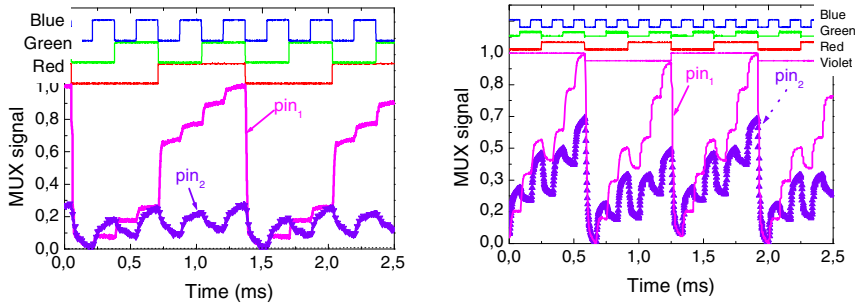

a) b)

Fig. 5. Filtered output signals under front (pin_1; lines) and back (pin_2; symbols) violet irradiation. a) Red, Green and Blue channels. b) Red, Green, Blue and violet channels. On the top of the figures the optical signals used to transmit the information guide the eyes.

Different gains for the RGB channels were obtained (Table 1). Due to this wavelength non-linearity under front violet background, the encoded multiplexed signal presents as many levels as the possible RGB combinations, in a maximum of 2^3 (eight-level encode).Those levels can be grouped into two main classes due to the high amplification of the red channel ($\alpha^V_{R,pin1}>>1$). The upper levels are ascribed to the presence of the red channel and the lower to its absence allowing the red channel decoder. Since under front irradiation the green channel is amplified ($\alpha^V_{G,pin1}>1$), the highest levels, in both classes, are ascribed to the presence of the green channel and the lower ones to its lack (long-pass filter). Under back irradiation the red channel is suppressed ($\alpha^V_{R,pin2}<<1$), the blue enhanced ($\alpha^V_{B,pin2}>1$) and the green reduced($\alpha^V_{G,pin2}<1$), so the encoded multiplexed signal presents a maximum of four separate levels (2^2). The highest levels correspond to the presence of the blue channel ON with or without the green ON respectively, and the other to its absence. The blue channel is then decoded using this simple algorithm (short-pass filter).

Results show that by means of violet optical bias control, the MUX photonic function may be modified, giving reconfiguration. This new method, based on wavelength background processing techniques enables the optical routing.

7 Conclusions

Integrated photonic filters based on SiC multilayer devices are analyzed and its transfer functions presented showing that the light-activated pi'n/pin a-SiC:H devices combine the demultiplexing operation with the simultaneous photodetection and self-amplification of an optical signal. Reconfiguration is provided by background wavelength control. Results show that the background wavelength and irradiation side control the output signal. By using background lights with complementary light penetration depths and changing the irradiation side, it is possible to change the spectral response and to filter a specific wavelength band acting either as a short- or a long- pass band filter or as a band-stop filter.

Acknowledgements. This work was supported by PTDC/EEA-ELC/111854/2009, PTDC/EEA-ELC/115577/2009 and PTDC/EEA-ELC/120539/2010.

References

1. Vieira, M., Louro, P., Fernandes, M., Vieira, M.A., Fantoni, A., Costa, J.: Three Transducers Embedded into One Single SiC Photodetector: LSP Direct Image Sensor, Optical Amplifier and Demux Device. In: Betta, G.F.D. (ed.) Advances in Photodiodes, ch. 19, pp. 403–425. InTech (2011) ISBN: 978-953-307-163-3
2. Louro, P., Vieira, M., Vieira, M.A., Fernandes, M., Costa, J.: Use of a SiC:H Photodiodes in Optical Communications Applications. In: Betta, G.F.D. (ed.) Advances in Photodiodes, ch. 19, pp. 377–402. InTech (2011) ISBN: 978-953-307-163-3
3. Iguchi, Y., Yamabayashi, N.: Novel rear-illuminated 1.55 μm-photodiode with high wavelength selectivity designed for bi-directional optical transceiver. In: Proc. 2nd Int. Conf. on InP and Related Mater, vol. 317, pp. 317–320 (2000)
4. Bas, M.: Fiber Optics Handbook, Fiber, Devices and Systems for Optical Communication, ch. 13. McGraw-Hill, Inc. (2002)
5. Randel, S., Koonen, A.M.J., Lee, S.C.J., Breyer, F., Garcia Larrode, M., Yang, J., Ng'Oma, A., Rijckenberg, G.J., Boom, H.P.A.: Advanced modulation techniques for polymer optical fiber transmission. In: ECOC 2007 (Th 4.1.4), Berlin, pp. 1–4 (2007)
6. Ashton, K.: That 'Internet of Things' Thing. RFID Journal (2012), http://www.rfidjournal.com/article/view/4986 (accessed October 27, 2012)
7. Vieira, M.A., Vieira, M., Costa, J., Louro, P., Fernandes, M., Fantoni, A.: Double Pin Photodiodes with Two Optical Gate Connections for Light Triggering: A Capacitive Two-phototransistor Mode. Sensors & Transducers Journal 10 (special issue), 96–120 (2011) ISSN: 1726-5479